JACS
JOURNAL OF THE AMERICAN CHEMICAL SOCIETY
Article
pubs.acs.org/JACS

Ligand Accessibility and Bioactivity of a Hormone−Dendrimer Conjugate Depend on pH and pH History

Sung Hoon Kim,[†] Zeynep Madak-Erdogan,[‡] Sung Chul Bae,[§] Kathryn E. Carlson,[†] Christopher G. Mayne,[†] Steve Granick,[§] Benita S. Katzenellenbogen,[‡] and John A. Katzenellenbogen*[,†]

[†]Department of Chemistry and [‡]Department of Molecular and Integrative Physiology, University of Illinois at Urbana−Champaign, Urbana, Illinois 61801, United States

[§]IBS Center for Soft and Living Matter and UNIST, Ulsan 689-798, South Korea

Supporting Information

ABSTRACT: Estrogen conjugates with a polyamidoamine (PAMAM) dendrimer have shown remarkably selective regulation of the nongenomic actions of estrogens in target cells. In response to pH changes, however, these estrogen−dendrimer conjugates (EDCs) display a major morphological transition that alters the accessibility of the estrogen ligands that compromises the bioactivity of the EDC. A sharp break in dynamic behavior near pH 7 occurs for three different ligands on the surface of a PAMAM-G6 dendrimer: a fluorophore (tetramethylrhodamine [TMR]) and two estrogens (17α-ethynylestradiol and diphenolic acid). Collisional quenching and time-resolved fluorescence anisotropy experiments with TMR−PAMAM revealed high ligand shielding above pH 7 and low shielding below pH 7. Furthermore, when the pH was cycled from 8.5 (conditions of ligand−PAMAM conjugation) to 4.5 (e.g., endosome/lysosome) and through 6.5 (e.g., hypoxic environment) back to pH 8.5, the 17α-ethynylestradiol− and diphenolic acid−PAMAM conjugates experienced a dramatic, irreversible loss in cell stimulatory activity; dynamic NMR studies indicated that the hormonal ligands had become occluded within the more hydrophobic core of the PAMAM dendrimer. Thus, the active state of these estrogen−dendrimer conjugates appears to be metastable. This pH-dependent irreversible masking of activity is of considerable relevance to the design of drug conjugates with amine-bearing PAMAM dendrimers.

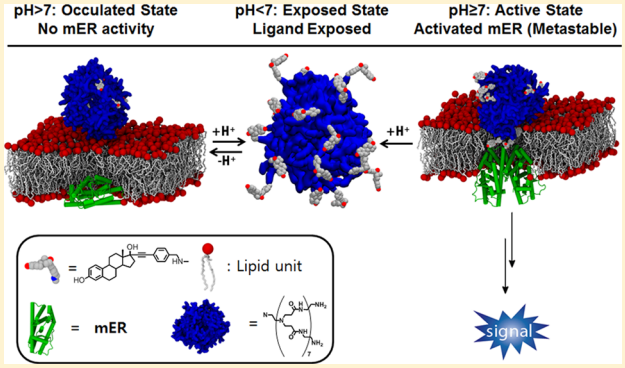

INTRODUCTION

Administration of exogenous estrogen agonists activates both extranuclear- and nuclear-initiated pathways of the estrogen receptor (ER) and results in global activation of ER in almost all target tissues. Because global activation of ER is often not clinically beneficial, a premium has been placed on the stimulation of ER activity in a tissue-selective manner.[1] One recently explored approach to this has involved pharmacological alteration of the balance of ER activation through the extranuclear versus nuclear signaling routes.[2,3] To activate selectively the extranuclear signaling pathway of ER, we designed and synthesized an "estrogen−dendrimer conjugate" (EDC) in which the estrogenic hormone 17α-ethynylestradiol (EE_2) is attached covalently to a sixth-generation (G6) polyamidoamine (PAMAM) dendrimer (Figure 1).[3,4]

In cell-based and in vivo studies, EDC showed remarkable selectivity, activating cytoplasmic kinase cascades without direct nuclear action,[2,3,5−10] modulating the dopamine receptor,[10] exerting neuroprotective effects,[11] regulating metabolic disease,[12−14] improving cortical bone mass,[15] participating in estrogen-mediated DNA repair,[16] and providing cardiovascular protection without stimulating reproductive organs (e.g., uterus) and breast cancers.[6,17] These results indicate that this polymer-based hormone conjugate exhibits a novel form of selective ER activation: Because of its size, EDC cannot enter the nucleus and thus cannot activate ER from nuclear sites. Consequently, it preferentially activates ER from membrane and cytoplasmic sites (ER present at these extranuclear locations will be designated mER.).[2,3] As a result of this restriction of its subcellular distribution, EDC activates through mER only a subset of estrogen-regulated responses, the bulk of which are beneficial, without activating reproductive tissues or breast cancer cells that would exacerbate the risk or promotion of cancer.

Some nanosized polymer−drug assemblies employ pH-responsive properties that enable them to effect selective antitumor drug delivery: they remain stable while they accumulate in tumors by the enhanced permeability−retention (EPR) effect, and they then release their active ingredient because of the low pH in the target zone[18] (extracellular tumor hypoxia, pH ∼6.5;[19−21] inflammatory tissue, ∼5.5;[22] lysosomes,

Received: June 8, 2015
Published: July 17, 2015

DOI: 10.1021/jacs.5b05952
J. Am. Chem. Soc. 2015, 137, 10326−10335

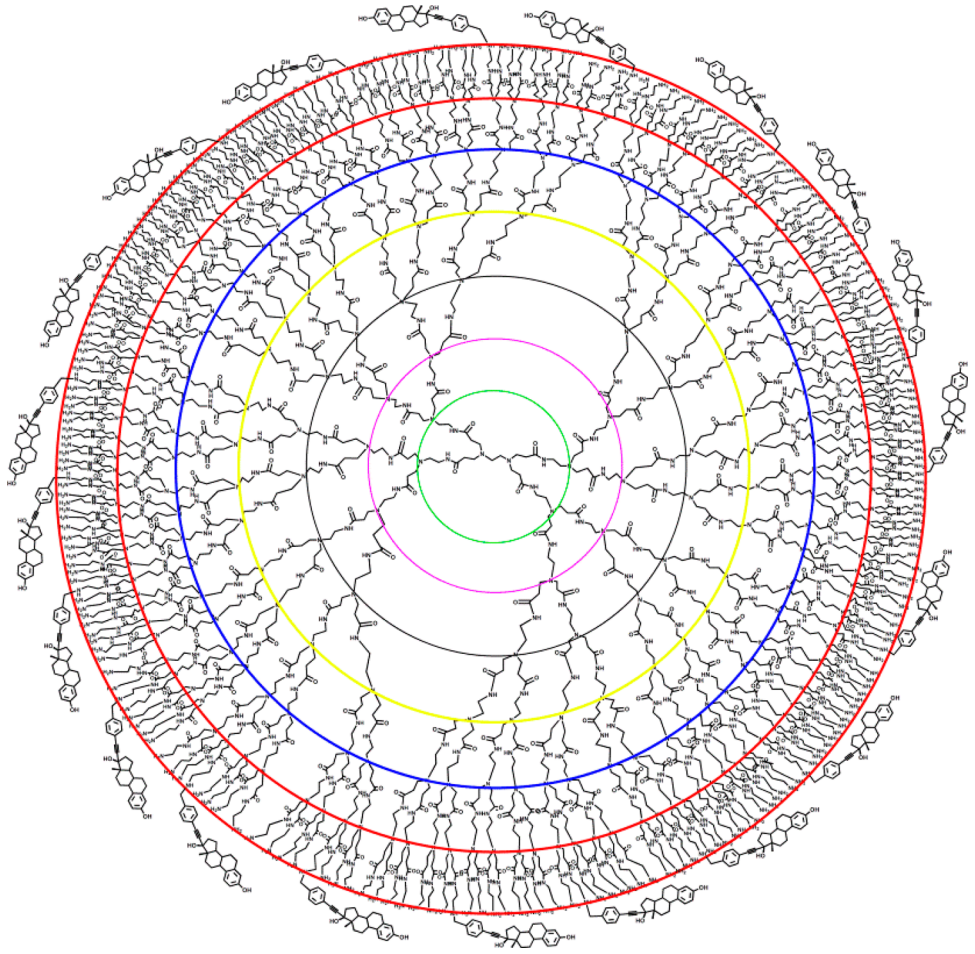

Figure 1. Full structure of the EDC consisting of 20 molecules of 17α-(4-phenylmethylene)ethynylestradiol conjugated to PAMAM G6.

~4.5[23]). Because it is robustly attached to the dendrimer by a stable covalent bond, however, the estrogen in the EDC cannot be released simply by a change in pH. Nevertheless, by affecting the conformation of the PAMAM, changes in pH might influence how accessible the estrogen is to the mER.

PAMAMs, which are becoming increasingly important as vehicles for medical drug delivery,[24−28] are ionizable dendrimeric polyamines; therefore, one would imagine them to show morphological changes—in size, shape, and internal volume—as a function of pH, reflecting the extent of protonation of their accessible surface/primary amines (pK_a = 7−9) versus their less basic internal/tertiary amines (pK_a = 3−6).[29−31] These predicted pH-dependent conformational changes of PAMAMs have been studied in considerable detail by molecular simulation,[17,32,33] from which one can surmise that amine-bearing PAMAM dendrimers undergo profound pH-dependent conformational changes over the physiological range of acidity (pH 4.5−7.4).

Little is known about the stability of these PAMAM conformational states or the functional relationship between these states and the accessibility and activity of bioactive ligands attached to a PAMAM dendrimer surface, all of which could affect the in vivo activity, selectivity, and utility of hormone−PAMAM conjugates. In particular, it is important to understand how the in vivo activity of a surface-tethered ligand might change over a pH range or even be affected in an irreversible manner by prior exposure to more acidic pH. We are aware of no prior comprehensive study exploring this issue.

Therefore, to probe the behavior of EDC-like PAMAM conjugates in cells and to assist in the design of new agents for future in vivo applications, in this work we investigated, through photophysical and spectroscopic methods and by multicolor subcellular-colocalization imaging and cell-based activity assays, the pH-dependent alteration of the accessibility and activity of hydrophobic molecules (a fluorophore and two estrogens) covalently attached to the surface of a G6 PAMAM dendrimer. To mimic the different pH environments that an EDC would encounter physiologically, these samples were preincubated at pH 4.5 (endosome/lysosome environment), 6.5 (hypoxic environment and tumor), 7.0, or 8.5 before being returned to pH 7.4 for cellular bioactivity and localization studies. These studies revealed remarkable pH-dependent alterations in EDC ligand motion and accessibility: initially, at the alkaline pH used for EDC preparation, the ligand was somewhat constrained but still accessible; then at acidic pH it became highly exposed and dynamic; and finally, after being returned to pH 7, the ligand became—unexpectedly—occluded by the collapsed dendrimeric PAMAM architecture and experienced *full loss of biological activity*. The effect of altered polymer conformations in response to exposure of the EDC to different pH conditions—and the pH history—that affect the flexibility and accessibility of pendant ligands on the PAMAM dendrimer surface could have profound consequences for the design and evaluation of other drug−polymer conjugates and their biomedical utility.

DOI: 10.1021/jacs.5b05952
J. Am. Chem. Soc. 2015, 137, 10326−10335

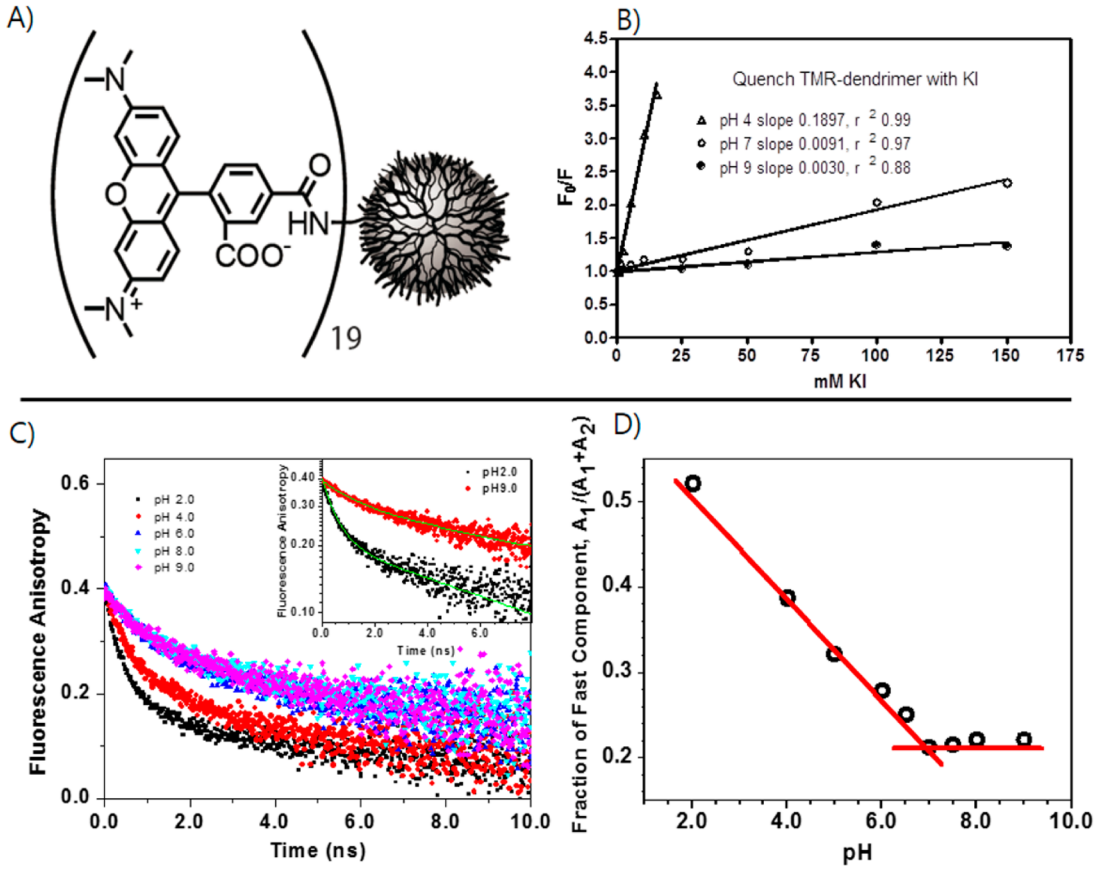

Figure 2. Collisional quenching by potassium iodide (KI) and time-resolved anisotropy measurements by time-correlated single-photon counting. (A) TMR-conjugated G6 PAMAM dendrimer. (B) Fluorescence from a $(TMR)_{19}$–PAMAM dendrimer (100 nM TMR-equivalent concentration) in MeOH was quenched by increasing concentrations of KI (0–150 mM). The emission intensity data were analyzed according to the Stern–Volmer equation, $F_0/F = 1 + K_{SV}[Q]$, before and after addition of KI, at pH 4, 7, and 9 (λ_{ex} = 541 nm, λ_{em} = 580 nm). (C) Representative time-resolved anisotropy measurements of TMR-conjugated G6 PAMAM dendrimer over the pH range 2–9. The inset shows the measurements at pH 2 and 9 fitted to a biexponential function, $y = A_1 \exp(-t/\tau_1) + A_2 \exp(-t/\tau_2) + y_0$, where τ_1 and τ_2, the fast and slow fluorescence decay times in nanoseconds, are considered to correspond to the local tumbling of individual TMR molecules and global tumbling of the whole PAMAM dendrimer and A_1 and A_2 are the respective populations of these states. (D) The ratio $A_1/(A_1 + A_2)$, where A_1 and A_2 designate the populations of the fast and slow motions of TMR, respectively, was plotted versus pH. (The detailed structure of the TMR–dendrimer conjugate and its preparation and characterization are given in Figures S3 and S5 in the Supporting Information.)

RESULTS

pH-Dependent Collisional Quenching and Time-Resolved Anisotropy of PAMAM G6 Dendrimer Conjugated to Tetramethylrhodamine, a Fluorescent Surrogate Ligand, Indicates Major Alterations in Ligand Exposure and Flexibility. To facilitate studies of how pH influences the PAMAM conformation and ligand accessibility, we used tetramethylrhodamine (TMR) as a fluorescent model ligand. We attached TMR covalently to the amine-terminated G6 ethylenediamine-core PAMAM dendrimer at the usual pH of 8.5, controlling the surface coverage to be 18–20 TMR molecules per dendrimer, similar to that of our EE_2-EDC compound (Figure 2A).[3,4]

We first explored the surface exposure of the dendrimer-bound TMRs by measuring the collisional fluorescence quenching effect of potassium iodide (KI).[34] The TMR–dendrimer conjugate was titrated with aqueous KI at three different pH values (Figure 2B). The quenching effect changed dramatically between pH 4 and 7, with the slope of the Stern–Volmer plot at pH 4 being 20-fold greater than that at pH 7.0; by contrast, the slope declined only 3-fold between pH 7 and 9. This suggests that as the pH is increased from 4 to 7, a marked change in dendrimer conformation occurs, progressively shielding the TMRs from exposure to KI; the conformational changes that occur between pH 7–9, however, result in only a moderate increase in ligand shielding.

This observation is interesting because the TMR–dendrimer conjugate was prepared at pH 8.5, conditions under which most surface/primary amines and inner/tertiary amines would be deprotonated. With little Coulombic repulsion to oppose it, the hydrophobic effect should force the dendrimer structure to collapse into a tightly compacted conformation, minimizing the volume and aqueous solvent-accessible surface of the more hydrophobic core.[31] Nevertheless, one might expect that the KI quencher would still have good accessibility to most of the TMRs on the dendrimer surface. Consequently, it was not clear why the quenching effect of KI at pH 9 would be so different from that at pH 4. These results led us to reconsider the accessibility—and potentially the activity—of hormonal ligands attached to the surface of a G6 PAMAM dendrimer as a function of the pH of the environment.

To further characterize the ligand conformation and accessibility, we used time-dependent fluorescence anisotropy to explore how the local motion of individual TMRs correlated

DOI: 10.1021/jacs.5b05952
J. Am. Chem. Soc. 2015, 137, 10326–10335

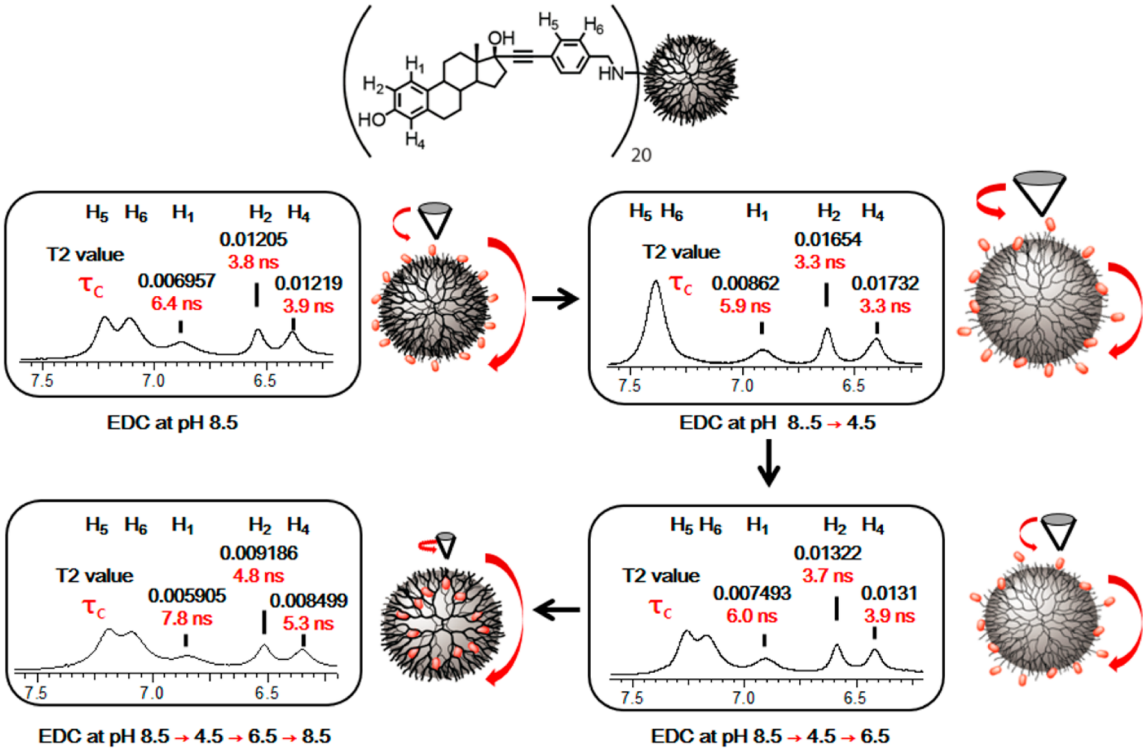

Figure 3. Rotational correlation time (τ_c) and spin−spin relaxation time (T_2) measurements. These describe the influence of ensemble movement and line broadening on the A ring of the estradiol moiety driven by small molecule−polymer interactions according to pH. Values of T_2 and τ_c are given above each peak in black and red, respectively. The size of the small red arrow and cone above the dendrimer cartoon indicates the degree of local tumbling; the size of the large red arrow to the right of the cartoon indicates the degree of global tumbling. The rotational correlation times were determined using the polynomial function τ_c (in ns) = $a_0 + a_1(R_2/R_1) + a_2(R_2/R_1)^2 + a_3(R_2/R_1)^3 + a_4(R_2/R_1)^4$, where $R_1/R_2 = T_2/T_1$ and the values for a_0, a_1, a_2, a_3, and a_4 were taken from the literature.[36]

with the global tumbling of the dendrimer. We adapted a time-correlated single-photon counting system[35] to measure the total anisotropy and deconvolute the local and global movements of TMRs attached to the dendrimer over the pH range from 2 to 9 (Figure 2C, D). Regardless of pH, the anisotropy decays displayed a biexponential pattern (Figure 2C): the fast-tumbling population (0.5−1.3 ns) was highest at pH 2, where it actually exceeded the slow-tumbling population (8.3−14.3 ns) (Figure 2D and Table S1 in the Supporting Information). At acidic pH, the PAMAM dendrimer would be highly protonated and thus because of Coulombic repulsion should favor a loose, extended conformation, providing room and flexibility for the TMRs at the ends of the dendrimer arms to tumble freely. The fraction of fast-moving species showed a progressive decrease with increasing pH until pH 7, beyond which this fraction did not change. Thus, in terms of TMR access to KI quenching and fast motion, pH 7 seems to be an important break point that divides looser, more flexible structural conformations of the amine-terminated G6 PAMAM dendrimer (below pH 7) from tighter, more rigid ones (above pH 7). These pH-dependent alterations of the PAMAM dendrimer conformation could alter the activity of bioactive ligands attached to this pH-responsive dendrimer.

Dynamic ^{1}H NMR Studies of EDC Highlight pH-Dependent Changes in Ligand Flexibility and a Transition to a Ligand-Buried State. To explore how the pH determines whether the bioactive estrogenic ligands (EE_2 and diphenolic acid [DPA]) attached to the EDC surface are either confined or accessible to the membrane ER (mER), we prepared an EE_2-EDC sample with 20 EE_2 molecules per dendrimer as usual at pH 8.5.[4] We then determined the rotational correlation times (τ_c) for the three aromatic A-ring protons of EE_2 on the surface of the EDC compound by measuring the spin−spin relaxation times (T_2) and spin−lattice relation times (T_1) after EDC exposure to different pH's in D_2O (Figure 3; for more detailed information, see Figure S2 and Table S2 in the Supporting Information). In each panel, the numbers indicate T_2 values as line widths at half-height (in black) and τ_c values (in red).[36] The measured rotational correlation times for each peak at different pH's reflect an ensemble movement averaged over the 20 EE_2 molecules on the surface of the G6 PAMAM dendrimer.

When the pH was lowered from 8.5 to 4.5, the τ_c values were 10−15% shorter than at the original pH of 8.5. The τ_c values became longer when the pH was raised back to 6.5, at which point they were similar to the original values at pH 8.5. Remarkably, when the EDC was taken through the full pH cycle from the original pH of 8.5 to pH 4.5 and then all the way back to pH 8.5, *the τ_c values became even 25−35% longer than they were originally at pH 8.5* (Figure S9 in the Supporting Information). This suggests that after the pH cycle, a larger number of the EE_2 ligands become confined within the dendrimer framework, thereby experiencing the more greatly retarded ensemble motion.

The associated T_2 values, which are inversely proportional to the line broadening experienced by a small molecule in the vicinity of a polymeric environment, showed a similar trend with the pH cycle of the EDC: the lines became narrower (longer T_2) at acidic pH, were as broad as they were *originally* at pH 8.5 when the pH was returned to pH 6.5, and then finally

DOI: 10.1021/jacs.5b05952
J. Am. Chem. Soc. 2015, 137, 10326−10335

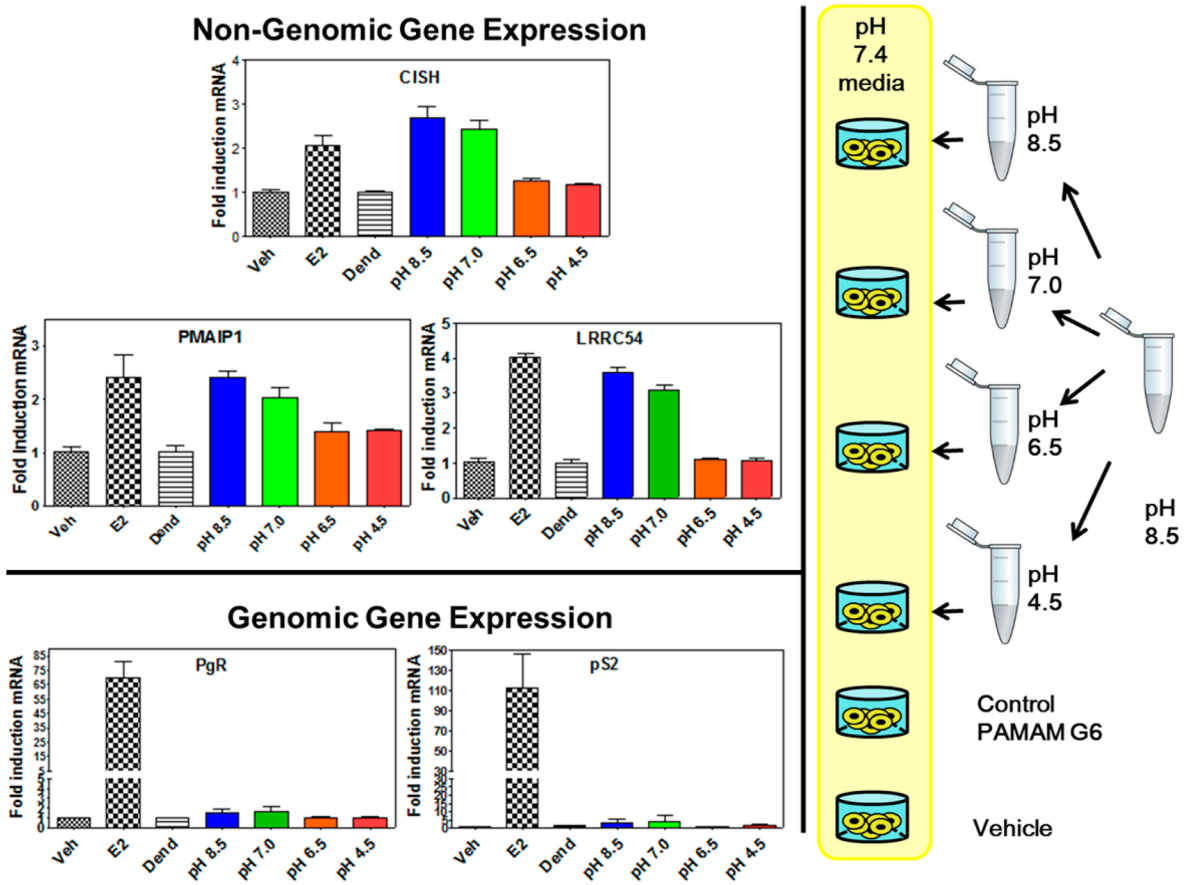

Figure 4. Gene expression in MCF-7 cells treated with 10 nM E_2 or EDC at an E_2-equivalent concentration of 10 nM. The nongenomic genes, CISH, PMAIP1, and LRRC54 (top), can be stimulated by estrogen receptor acting at extranuclear sites, so both E_2 and EDC are active. The genomic genes, PgR and pS2, can be stimulated only by nuclear activity of the estrogen receptor (bottom), so only E_2 is active. Legend: Veh, vehicle-treated control cells; E2, cells treated with estradiol (10 nM); Dend, cells treated with underivatized control G6 PAMAM dendrimer; pH 8.5, 7.0, 6.5, and 4.5, cells treated with EDC samples that had been exposed to different pH conditions.

were even broader (shorter T_2) when the pH was raised back to pH 8.5. This behavior is again consistent with the motion of the surface ligands becoming more constrained by being caught within the interior of the polymer after the cycle through acidic pH.

Both the fluorescence anisotropy and dynamic NMR experiments indicate that pH-dependent alterations of the dendrimer framework influence the flexibility of pendant ligands (either TMR or EE_2) on the surface of the G6 PAMAM dendrimer. The key observation made from measuring the τ_c and T_2 values through a pH cycle is that *after cycling of the EDC from pH 8.5 to pH 4.5 and then back to pH 8.5, the EE_2 ligands that were originally on the PAMAM surface and accessible appeared to become more buried within the PAMAM skeleton than before*. This change could have a significant effect on the ligand activity, and it suggests that the EDC as initially prepared at pH 8.5 is in an active but metastable conformational state that, after being cycled to pH 4.5 and then back to 8.5, undergoes further conformational changes that bury the ligands and render the EDC inactive.

Gene Expression Patterns for EDC and the DPA–Dendrimer Conjugate Are Affected by Prior Exposure to Different pH. These observations prompted us to investigate the biological activity of EDC in a cellular context as a function of its "pH history". An EDC sample prepared at pH 8.5 was split into four aliquots, which were either maintained at pH 8.5 or adjusted to pH 7.0, 6.5, or 4.5. After a period of time (1 h to 1 day), a small portion of each sample was then returned to pH 7.4 by being diluted ~10 000-fold into pH 7.4 tissue culture medium containing human breast cancer (MCF-7) cells. The levels of expression of five representative genes were then determined for each of the EDC preparations having differing pH histories (Figure 4). Three of these genes (CISH, PMAIP1, and LRRC54; Figure 4, top panels) are known to be driven by the extranuclear action of mER (termed "nongenomic" activity) and are effectively stimulated by EDC prepared under the conventional high-pH protocol and by estradiol (E_2), whereas two of these genes (PgR and pS2; Figure 4, bottom panels) are known to require direct nuclear-initiated ER action (termed "genomic" activity) and are stimulated by E_2 but not by EDC.[3,8] MCF-7 cells were treated with each EE_2-EDC sample (10 nM EE_2-equivalent concentration) at pH 7.4 for 4 h, and the level of gene expression was determined by real-time polymerase chain reaction (PCR) analysis.

As expected, none of the EDC samples stimulated the genomic genes (Figure 4, bottom).[8] Notably, while the EDC originating from the pH 7.0 and pH 8.5 samples stimulated the nongenomic genes effectively (Figure 4, top), the EDC samples that had been exposed to pH 4.5 and 6.5 (but like the others were moved back to pH 7.4 prior to the assay) had essentially no effect on nongenomic gene expression, giving the same response as vehicle or control (underivatized) G6 PAMAM.

DOI: 10.1021/jacs.5b05952
J. Am. Chem. Soc. 2015, 137, 10326–10335

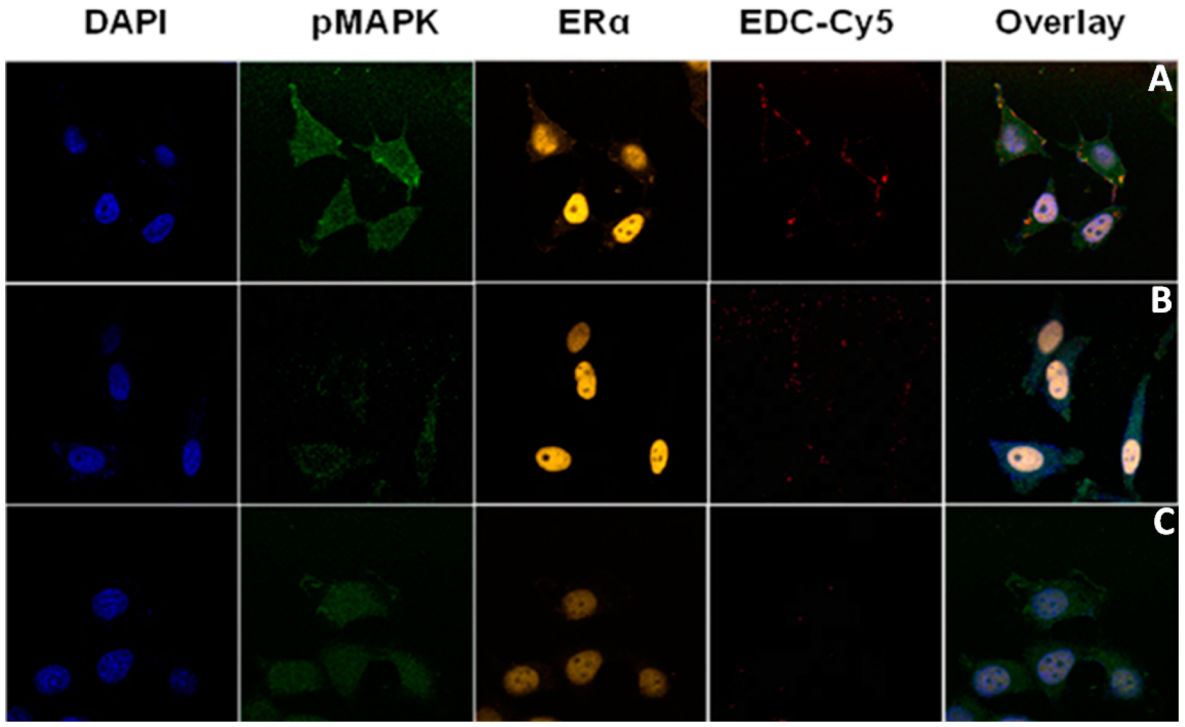

Figure 5. Multicolor fluorescence microscopic imaging to visualize the colocalization of Cy5-labeled EDC (Cy5-EDC), ERα, and pMAPK. A. Colocalization of Cy5-EDC maintained at pH 8.5. Cy5-EDC (red), ERα (Alexa-568, yellow), and pMAPK (Alexa-488, green). B. Colocalization of Cy5-EDC exposed to pH 6.5. C. Colocalization of control Cy5-PAMAM G6 control dendrimer compound maintained at pH 8.5. Each EDC was incubated at 1 μM (ligand equivalent) with MCF-7 cells for 15 min at 37 °C for images A, B. Cy5-PAMAM G6 dendrimer at 50 nM was treated to get image C. The same amounts of ERα and pMAPK antibody were used to get image A, B, and C. ERα and pMAPK antibody were labeled with Alexa-568 and Alexa-488, respectively. Columns (left to right) display the location of the nuclei (DAPI), pMAPK, ERα, EDC, and an overlay, respectively. All images were taken at 60× magnification.

(The loss of EDC activity on the nongenomic genes was not due to loss of ligand by cycling to acidic pH, as no loss of ligand was observed in the dynamic NMR studies or by mass spectrometric analysis of EDC before and after pH cycling [Figure S6 in the Supporting Information].) The more hydrophilic DPA−dendrimer conjugate (DPA-DC), which was studied to evaluate the generality of this phenomenon, gave very similar results, activating nongenomic genes when kept at high pH but not when cycled through low pH and back prior to cellular assays (Figure S7 in the Supporting Information).

Notably, the pH 7 cutoff in EDC-stimulated expression of the nongenomic genes nicely matches the pH 7 cutoffs found in the fluorescence quenching and anisotropy experiments (Figure 2B−D). Furthermore, our findings that the pattern of gene expression depends on the pH history of the EDC or DPA-DC preparation are consistent with the results of the NMR rotational correlation time experiments, through which we found that cycling EDC through acidic pH causes ligands to transition from a higher-motion surface-exposed state to a lower-motion buried or occluded state.

Cellular Imaging Provides Further Evidence for the Effect of the pH History on EDC Cellular Activity and Colocalization. To further explore the impact of the pH history on the biological function of EDC and DPA-DC, we monitored activation of the MAPK cascade, a well-recognized action of estrogens through mER,[3,8] and we determined the colocalization of ERα with activated pMAPK1/2 using fluorescence microscopy. Cells treated with Cy5-labeled EDC (Cy5-EDC) that had been stored at pH 8.5 (but were examined at pH 7.4) showed intense signals from ERα (yellow, largely nuclear) and pMAPK1/2 (green, largely cytoplasmic). Because only 5−10% of ERα resides close to the cell membrane,[37] the Cy5-EDC signal (red) appeared as punctate perimembrane spots (as seen before[2,3]), and these were colocalized with a subfraction of both ERα and pMAPK (Figure 5A). By contrast, the EDC samples that had been exposed to pH 6.5 caused minimal activation of pMAPK1/2 and showed minimal colocalization with ERα and pMAPK1/2 (Figure 5B).

Control experiments in the presence and absence of Cy5-labeled PAMAM G6 dendrimer without any ligand (Figure 5C) showed clearly that the MAPK activation and colocalization observed in Figure 5A are ligand-dependent phenomena. In addition, colocalization of Cy5-DPA-DC (DPA being a ligand structurally similar to TMR; Figure S3 in the Supporting Information) showed the same behavior as EDC: Cy5-DPA-DC maintained at pH 8.5 colocalized with ERα and pMAPK1/2, but Cy5-DPA-DC exposed to pH 6.5 did not (Figure S8 in the Supporting Information).

Proximity ligation assays[38] were used to examine with higher spatial sensitivity whether the colocalized perimembrane speckles seen in Figures 5A and S8 represent real interactions among ERα, pMAPK, and EDC (or DPA-DC) (Figure 6). The strong speckled signals (correlation histogram in Figure 6 left, bottom panel), attributed to the ligation product of ERα interacting with pMAPK1/2, were exactly congruent with the signals for EDC outside the nucleus (Figure 6 left, middle panel; the top panel shows an overlay), providing further evidence that the multiple ligands on the dendrimer surface are

DOI: 10.1021/jacs.5b05952
J. Am. Chem. Soc. 2015, 137, 10326−10335

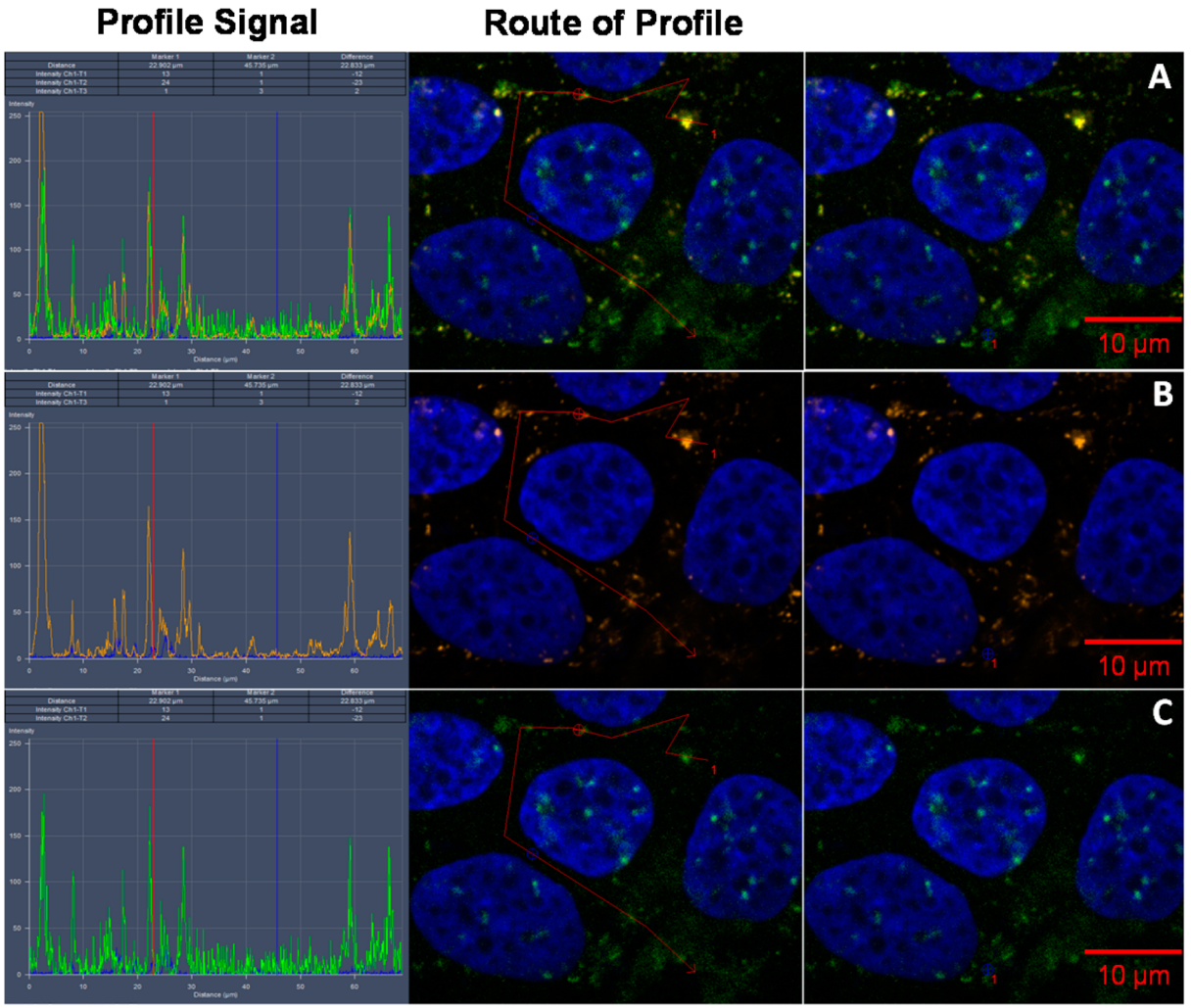

Figure 6. Confocal microscopy imaging for the proximity ligation assay (PLA). PLA highlights the close interaction among ERα, pMAPK, and TMR-labeled EDC (TMR-EDC) in the extranuclear cellular area, thought to result in the initiation of kinase-cascade signal transduction. The *y* axis of each histogram (left column) indicates the signal intensity at the corresponding location (*x* axis) along the red-line track drawn in the picture (middle column). The top row (A) shows the overlay of the images of TMR-EDC (red), DAPI (blue; nucleus), and the PLA signal from the proximity-ligated ERα–pMAPK complex (green). The middle row (B) and bottom row (C) show the localization of TMR-EDC and the ERα–pMAPK complex, respectively. TMR-EDC maintained at pH 8.5 as prepared was added to MCF-7 cells for 45 min, and the proximity ligation assay was performed.

able to activate ERα outside the nucleus, promoting its interaction with pMAPK1/2 to initiate a kinase cascade.

Overall then, the striking correspondence relating kinase activation, EDC/ERα/pMAPK1/2 colocalization, and patterns of gene expression for the EDC samples provide further evidence that the surface ligands retain good activity in EDC samples not exposed to acidic conditions but that an excursion through acidic pH and return to physiological conditions causes the surface ligands to become confined within the interior of the PAMAM dendrimer (as supported by the dynamic NMR studies), resulting in loss of their biological activity.

DISCUSSION

Using spectroscopic analyses, cellular bioactivity assays, and subcellular microscopic imaging, we have demonstrated that pH cycling of EDC from normal physiological pH to acidic pH and back again causes the ligand to become buried within the hydrophobic core of the dendrimer, occluding it from interaction with mER and thereby eliminating its biological activity. While pH-induced aggregation of the EDC rather than ligand occlusion might in principle account for all or some of this loss of biological activity, using dynamic light scattering (DLS) measurements we found essentially no change in the hydrodynamic diameter of the EDC as a result of prior exposure to acidic pH (Figure S10 in the Supporting Information). Hence, ligand occlusion rather than aggregation appears to be the most likely mechanism to account for the loss of EDC biological activity resulting from cycling to low-pH conditions.

A schematic representation of the three states of the EDC at different pH's and their potential interactions with a membrane bilayer and mER, developed by molecular dynamics simulations and drawn to scale, is given in Figure 7. At the pH of EDC synthesis (8.5), the largely deprotonated G6 PAMAM is compact and condensed, yet its surface amines are able to react efficiently with the derivatizing reagent for EE_2 or other ligands, producing hormone–dendrimer conjugates having ligands that are external (blue, PAMAM; gray/red, EE2; Figure 7 right) though not very mobile (little fast motion in the anisotropy experiment) or well-exposed to quenching by KI. This state can

DOI: 10.1021/jacs.5b05952
J. Am. Chem. Soc. 2015, 137, 10326–10335

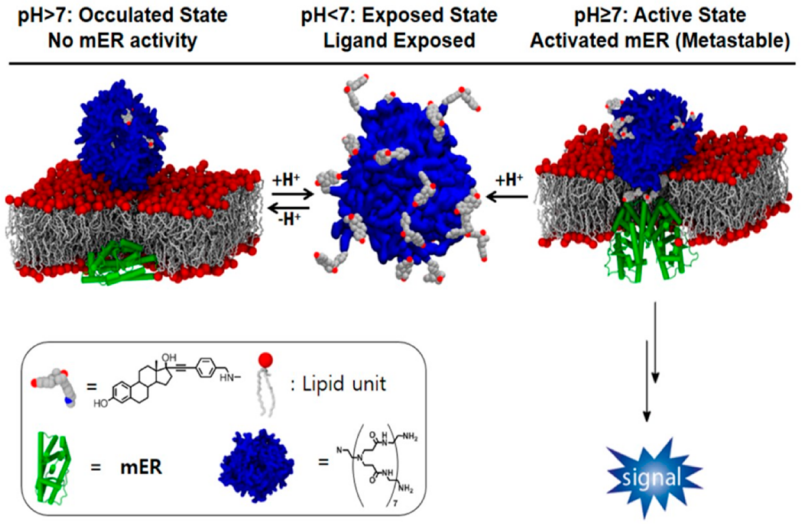

Figure 7. Schematic representation of the three states of the EDC and interactions with membrane ER and a membrane bilayer. The "surface-compact state" (right) is the active but metastable form produced only during EDC synthesis at pH 8.5. In this state the ligands are held close to the surface of the PAMAM dendrimer, and they display some mobility, experience limited fluorescence quenching, and can be accessed by the fraction of estrogen receptors that control nongenomic gene expression (designated as membrane ER or mER). In the "expanded state" of the EDC (middle), which forms at low pH (4.5, 6.5), the ligands are extended, giving them mobility and exposing them to active quenching, but the cell activity cannot be assayed at these acidic pH values. Returning the expanded state to pH 7.4 for cell-based assays results in a transition to the "occluded state" (left), which is more stable than the surface-compact state. In the occluded state, the lipophilic ligands become entrapped in the more lipophilic interior of the PAMAM dendrimer and cannot be accessed by the mER. (All three elements, the EDC, membrane, and mER [ligand binding domain], were generated by molecular modeling and are represented at relative scale in the left and right images. Details of modeling and skeletal representations of EDC and DPA-DC are given in Figures 1 and S1).

be termed "surface-compact", and it appears to be the initial state of the conjugates after preparation and also when they are moved only to pH 7.4, the condition of the cell assays for all of the EDCs. Upon interaction with the cell membrane, the hydrophobic ligands on the surface-compact form of the EDC are sufficiently exposed that they can be accessed by the cytoplasmic or membrane fraction of estrogen receptor (mER, green), an interaction that results in the activation of protein kinase cascades leading to expression of nongenomic genes; this interaction might involve or be followed by endocytosis.

By contrast, when the surface-compact form of the EDC is exposed to acidic conditions (pH 6.5 and especially pH 4.5), it undergoes a pronounced conformational change to an "expanded" form in which Coulombic repulsion between the highly protonated amines expands the dendrimer volume, extending the arms bearing the ligands (Figure 7 middle). In this state, the ligands undergo rapid local tumbling and are very accessible to KI quenching.

When the expanded form of the EDC is returned to pH 7.4 by being diluted into the cell assay medium at this pH, it does not return to the original surface-compact form. Rather, we propose that when the dendrimer is in the expanded state, the lipophilic EE_2 ligands have, for the first time, an opportunity to explore the more hydrophobic interior of the PAMAM dendrimer. With rising pH, during the process of dendrimer recondensation, the lipophilic ligands become trapped in the dendrimer interior, forming what can be termed an "occluded" state of the EDC (Figure 7 left). In this occluded state, the sequestered ligands are not able to access the mER (the gray/red ligands are less visible in Figure 7 left); thus, this form of the EDC shows little cellular activity. With lipophilic ligands like EE_2, it is likely that the occluded state is more stable than the surface-compact state because the lipophilic ligand, given the opportunity, prefers to reside in the more hydrophobic core of the PAMAM than on the more polar dendrimer surface.

This three-state model for the conformation and activity of EDC-like drug–PAMAM dendrimer conjugates suggests that such molecules might be engineered to have other unusual forms of selectivity. Nanosized PAMAM covalent conjugates of cytotoxic drugs could first be induced to adopt the occluded state by cycling through acidic pH and thus would have low activity on normal cells. Dendrimers that become trapped in tumors by the EPR effect,[39,40] however, would adopt the extended conformation in response to the local acidic environment of the tumor or in acidified vesicles after endocytosis, exposing tumor cells selectively to the cytotoxic effect of the drug. Other approaches to regulate extracellular versus intracellular activity of drug–PAMAM dendrimer conjugates can be envisioned.

CONCLUSIONS

We have elucidated the behavior of ligands tethered to the surface of amine-bearing G6 PAMAM dendrimers using TMR as a fluorescent ligand surrogate for the bioactive hormone, ethynylestradiol (EE_2). This enabled us to evaluate ligand exposure by fluorescence quenching and ligand motion by time-domain fluorescence polarization. In addition, measurement of rotational correlation times (τ_c) and spin–spin relaxation times (T_2) of EDC itself provided information on global changes in the population of surface-bound hormone, indicating whether they are accessible, extended, or occluded as a function of pH or pH history. The greater mobility and exposure of the ligand at acidic pH, together with the high activity of the EDC prepared and maintained at alkaline pH versus the low activity of EDCs that were cycled through low pH, are consistent with a three-state model for EDC conformation in which selective activity in stimulating non-

DOI: 10.1021/jacs.5b05952
J. Am. Chem. Soc. 2015, 137, 10326–10335

genomic gene responses in target cells is mediated only by the ligand-accessible, surface-compact, active form of EDC. Notably, this form is metastable and can be induced to relax, resulting in an occluded, inactive state, by cycling through acidic pH. This model should provide a useful guide for the design and evaluation of other drug−PAMAM dendrimer conjugates.

EXPERIMENTAL SECTION

Materials and Methods. ^{1}H and ^{13}C NMR spectra were recorded on a Varian Inova-500 spectrometer with D_2O. Matrix-assisted laser desorption ionization time of flight (MALDI-TOF) mass spectrometry (with 2,5-dihydroxybenzoic acid [DHB] as a matrix) and electrospray ionization mass spectrometry were performed using Voyager-DE STR (Applied Biosystems) and Q-TOF Ultima API (Waters) spectrometers, respectively Fluorescence experiments used a Spex Fluorolog II (model IIIc) cuvette-based fluorometer with Data Max 2.2 software (Spex Industries, Edison, NJ). All of the data were analyzed with Origin 7.5 (OriginLab, Northampton, MA) and Prism 5.0 (GraphPad Software, San Diego, CA). Compounds and materials were obtained from the sources indicated: diphenolic acid (TCI America, Montgomeryville, PA), ethylenediamine-core amine-terminated G6 PAMAM dendrimer (Aldrich, St. Louis, MO), and TMR-NHS ester (Berry & Associates, Dexter, MI).

TMR-Conjugated PAMAM Dendrimer. To a solution of ethylenediamine-core G6 PAMAM dendrimer (86 nmol, 5 mg, 100 mg 5% in 400 μL of MeOH) was added TMR-NHS ester (2.06 μmol, 1.09 mg in 50 μL of DMF) in MeOH, and the mixture was continuously stirred for 1 h. The reaction mixture was transferred into 3 mL of 30k cutoff Amicon filter (Millipore) and diluted with water (2 mL) before being centrifuged multiple times (466 *g*) to eliminate free ligand. The pellet liquid was transferred into a small vial and dried to give a film of a viscous liquid, which was kept under nitrogen and used to make a stock solution (~15 mM TMR or DPA equivalent) in methanol. The pH of a small aliquot was adjusted with 5 N or 0.1 N HCl and 5 N or 0.1 N NaOH by microtitration on the basis of the assumption that 510 total inner tertiary and outer primary amines remain in the PAMAM G6 dendrimer after ligand conjugation. All of the data were analyzed with Origin 7.5.

KI Quenching Experiments. Potassium iodide quenching experiments used a Spex Fluorolog II (model IIIc) cuvette-based fluorometer with Data Max 2.2 software. Excitation was at 541 nm and emission at 580 nm. Aliquots of the TMR−dendrimer conjugate at a TMR-equivalent concentration of 100 nM in MeOH were adjusted to pH 4, 7, and 9 and then titrated with 0−150 mM KI (in 10 mM $Na_2S_2O_3$).

Time-Resolved Fluorescence Anisotropy Measurements. Fluorescence anisotropy was measured with a home-built time-correlated single-photon counting system. Two-photon excitation of the fluorescent probe molecules was induced using a femtosecond Ti:sapphire laser (Tsunami, Spectra-Physics) with a pulse width of 100 fs. The repetition rate was 80 MHz, and the wavelength was 800 nm. Fluorescence was excited and collected by the same objective lens (LD-Neofluar, NA = 0.7, Carl Zeiss) at confocal geometry. The fluorescence signal was split into two perpendicular polarizations and monitored simultaneously by two fast avalanche photodiodes (id100−50, IDQ). Details of the experimental setup are described elsewhere.[35]

Rotational Correlation Time Measurement by NMR Spectroscopy. EDC with ~20 conjugated EE_2 (32 mg) was dissolved in 0.65 mL of D_2O, and then the pH was adjusted with 35 wt % 0.1 N DCl in D_2O and 40 wt % 0.1 N NaOD in D_2O using a microsyringe on the basis of the total number of amines on the dendrimer. (pH values were confirmed by pH indicator paper; nonbleeding pH 5.0 to 10.0, MColorpHast, EMD Millipore) To minimize magnetic field inhomogeneity, spectra were obtained from the same NMR tube. T_1 and T_2 values were determined on a Varian Unity-500 narrow-bore NMR spectrometer by means of a Hahn echo decay experiment and an inversion−recovery method, respectively, using internally installed software. Correlation times were determined using the polynomial function τ_c (in ns) = $a_0 + a_1(R_2/R_1) + a_2(R_2/R_1)^2 + a_3(R_2/R_1)^3 + a_4(R_2/R_1)^4$, where $R_1/R_2 = T_2/T_1$ and the values of a_0, a_1, a_2, a_3, and a_4 were taken from the literature.[36]

Cell Culture, RNA Extraction, and Real-Time PCR Analysis of Gene Expression Regulation. MCF-7 human breast cancer cells, which contain high levels of ERα, were maintained in culture as previously described.[41] At 6 days before E_2 treatment, the cells were switched to phenol red-free medium containing charcoal-dextran-treated calf serum. The medium was changed on day 2 and day 4 of culture, and the cells were then treated with 10 nM E_2 or EDC at an E_2-equivalent concentration of 10 nM for 4 h. After cell treatments, total RNA was isolated, reverse-transcribed, and analyzed by real-time PCR as described previously.[41] Primers for the estrogen-regulated genes CISH, PMAIP1, LRRC54, PgR, and pS2 have been described previously.[3,8]

Immunofluorescence Microscopy for Colocalization Studies. MCF-7 cells were treated for 15 min with Cy5-labeled EDC, which had been stored at the indicated pH, and Cy5-labeled empty dendrimer. Cells were then washed in phosphate-buffered saline (PBS), fixed on glass coverslips in 4% paraformaldehyde for 30 min, and washed two times for 5 min in PBS. After incubation in acetone for 5 min, another PBS wash was performed, and then cells were incubated with ERα antibody (F10, Santa Cruz Biotechnology) and pMAPK1/2 antibody (9101, Cell Signaling) overnight. The cells were then incubated with goat anti-mouse Alexa-568 and goat anti-rabbit Alexa-488 secondary antibodies. These slides were mounted and stained using Prolong Gold antifade with 4,6-diamidino-2-phenylindole (DAPI) (Molecular Probes) to identify the nuclei. Samples were observed with an LSM 710 confocal microscope, and fluorescence images (20 optical sections per cell) were collected and overlaid using ZEN 2011 software.

Proximity Ligation Assay. The proximity ligation assay (PLA) was performed using the Duolink In Situ Kit (Olink Bioscience) according to the manufacturer's instructions. Briefly, cells were treated and prepared similar to immunofluorescence methods. Overnight incubation with primary antibodies was followed by hybridization with two PLA probes at 37 °C for 1 h and then by ligation for 15 min and amplification for 90 min at 37 °C. A coverslip was mounted on the slide after PLA to acquire and analyze images as above.

ASSOCIATED CONTENT

Supporting Information

Molecular modeling, full structure of EDC, proton NMR spectra of EDC at different pH, synthesis of DPA−dendrimer conjugate, gene expression data and colocalization microscopy picture for DPA−dendrimer, and an analysis of T_1 and T_2. The Supporting Information is available free of charge on the ACS Publications website at DOI: 10.1021/jacs.5b05952.

AUTHOR INFORMATION

Corresponding Author

*jkatzene@illinois.edu

Notes

The authors declare no competing financial interest.

ACKNOWLEDGMENTS

We are grateful for support of this research through grants from the U.S. Department of Energy, Division of Materials Science (fluorescence anisotropy measurements supported by DEFG02-02ER46019 to S.G.), the Institute for Basic Science, Project Code IBS-R020-D1 to S.G.), and the U.S. National Institutes of Health (PHS 5R37DK015556 to J.A.K.). NMR spectra were obtained in the Varian Oxford Instrument Center for Excellence in NMR Laboratory at the University of Illinois.

DOI: 10.1021/jacs.5b05952
J. Am. Chem. Soc. 2015, 137, 10326−10335

REFERENCES

(1) Maximov, P. Y.; Lee, T. M.; Jordan, V. C. *Curr. Clin. Pharmacol.* **2013**, *8*, 135.
(2) Chambliss, K. L.; Wu, Q.; Oltmann, S.; Konaniah, E. S.; Umetani, M.; Korach, K. S.; Thomas, G. D.; Mineo, C.; Yuhanna, I. S.; Kim, S. H.; Madak-Erdogan, Z.; Maggi, A.; Dineen, S. P.; Roland, C. L.; Hui, D. Y.; Brekken, R. A.; Katzenellenbogen, J. A.; Katzenellenbogen, B. S.; Shaul, P. W. *J. Clin. Invest.* **2010**, *120*, 2319.
(3) Harrington, W. R.; Kim, S. H.; Funk, C. C.; Madak-Erdogan, Z.; Schiff, R.; Katzenellenbogen, J. A.; Katzenellenbogen, B. S. *Mol. Endocrinol.* **2006**, *20*, 491.
(4) Kim, S. H.; Katzenellenbogen, J. A. *Angew. Chem., Int. Ed.* **2006**, *45*, 7243.
(5) Chakravarty, D.; Nair, S. S.; Santhamma, B.; Nair, B. C.; Wang, L.; Bandyopadhyay, A.; Agyin, J. K.; Brann, D.; Sun, L.-Z.; Yeh, I.-T.; Lee, F. Y.; Tekmal, R. R.; Kumar, R.; Vadlamudi, R. K. *Cancer Res.* **2010**, *70*, 4092.
(6) Fan, P.; Griffith, O. L.; Agboke, F. A.; Anur, P.; Zou, X.; McDaniel, R. E.; Creswell, K.; Kim, S. H.; Katzenellenbogen, J. A.; Gray, J. W.; Jordan, V. C. *Cancer Res.* **2013**, *73*, 4510.
(7) Kousteni, S.; Almeida, M.; Han, L.; Bellido, T.; Jilka, R. L.; Manolagas, S. C. *Mol. Cell. Biol.* **2007**, *27*, 1516.
(8) Madak-Erdogan, Z.; Kieser, K. J.; Kim, S. H.; Komm, B.; Katzenellenbogen, J. A.; Katzenellenbogen, B. S. *Mol. Endocrinol.* **2008**, *22*, 2116.
(9) Adlanmerini, M.; Solinhac, R.; Abot, A.; Fabre, A.; Raymond-Letron, I.; Guihot, A. L.; Boudou, F.; Sautier, L.; Vessieres, E.; Kim, S. H.; Liere, P.; Fontaine, C.; Krust, A.; Chambon, P.; Katzenellenbogen, J. A.; Gourdy, P.; Shaul, P. W.; Henrion, D.; Arnal, J. F.; Lenfant, F. *Proc. Natl. Acad. Sci. U. S. A.* **2014**, *111*, E283.
(10) Alyea, R. A.; Laurence, S. E.; Kim, S. H.; Katzenellenbogen, B. S.; Katzenellenbogen, J. A.; Watson, C. S. *J. Neurochem.* **2008**, *106*, 1525.
(11) Yang, L.-c.; Zhang, Q.-G.; Zhou, C.-f.; Yang, F.; Zhang, Y.-d.; Wang, R.-m.; Brann, D. W. *PLoS One* **2010**, *5*, e9851.
(12) Tiano, J. P.; Delghingaro-Augusto, V.; Le May, C.; Liu, S.; Kaw, M. K.; Khuder, S. S.; Latour, M. G.; Bhatt, S. A.; Korach, K. S.; Najjar, S. M.; Prentki, M.; Mauvais-Jarvis, F. *J. Clin. Invest.* **2011**, *121*, 3331.
(13) Tiano, J. P.; Mauvais-Jarvis, F. *Endocrinology* **2012**, *153*, 2997.
(14) Wong, W. P. S.; Tiano, J. P.; Liu, S.; Hewitt, S. C.; Le May, C.; Dalle, S.; Katzenellenbogen, J. A.; Katzenellenbogen, B. S.; Korach, K. S.; Mauvais-Jarvis, F. *Proc. Natl. Acad. Sci. U. S. A.* **2010**, *107*, 13057.
(15) Bartell, S. M.; Han, L.; Kim, H.-n.; Kim, S. H.; Katzenellenbogen, J. A.; Katzenellenbogen, B. S.; Chambliss, K. L.; Shaul, P. W.; Roberson, P. K.; Weinstein, R. S.; Jilka, R. L.; Almeida, M.; Manolagas, S. C. *Mol. Endocrinol.* **2013**, *27*, 649.
(16) Li, Z.; Chen, K.; Jiao, X.; Wang, C.; Willmarth, N. E.; Casimiro, M. C.; Li, W.; Ju, X.; Kim, S. H.; Lisanti, M. P.; Katzenellenbogen, J. A.; Pestell, R. G. *Cancer Res.* **2014**, *74*, 3959.
(17) Liu, Y.; Bryantsev, V. S.; Diallo, M. S.; Goddard Iii, W. A. *J. Am. Chem. Soc.* **2009**, *131*, 2798.
(18) Nowag, S.; Haag, R. *Angew. Chem., Int. Ed.* **2014**, *53*, 49.
(19) Chiche, J.; Ilc, K.; Laferrière, J.; Trottier, E.; Dayan, F.; Mazure, N. M.; Brahimi-Horn, M. C.; Pouysségur, J. *Cancer Res.* **2009**, *69*, 358.
(20) Frechet, J.; Schuerch, C. *J. Am. Chem. Soc.* **1969**, *91*, 1161.
(21) Švastová, E.; Hulíková, A.; Rafajová, M.; Zaťovičová, M.; Gibadulinová, A.; Casini, A.; Cecchi, A.; Scozzafava, A.; Supuran, C. T.; Pastorek, J. r.; Pastoreková, S. *FEBS Lett.* **2004**, *577*, 439.
(22) Steen, K. H.; Steen, A. E.; Reeh, P. W. *J. Neurosci.* **1995**, *15*, 3982.
(23) Mindell, J. A. *Annu. Rev. Physiol.* **2012**, *74*, 69.
(24) Esfand, R.; Tomalia, D. A. *Drug Discovery Today* **2001**, *6*, 427.
(25) Kitchens, K. M.; Ghandehari, H. In *Nanotechnology in Drug Delivery*; de Villiers, M. M., Aramwit, P., Kwon, G. S., Eds.; Biotechnology: Pharmaceutical Aspects, Vol. *X*; Springer: New York, 2009; p 423.
(26) Yellepeddi, V. K.; Kumar, A.; Palakurthi, S. *Anticancer Res.* **2009**, *29*, 2933.
(27) Kannan, R. M.; Nance, E.; Kannan, S.; Tomalia, D. A. *J. Intern. Med.* **2014**, *276*, 579.
(28) Tomalia, D. A.; Christensen, J. B.; Boas, U. *Dendrimers, Dendrons, and Dendritic Polymers: Discovery, Applications, and the Future*; Cambridge University Press: Cambridge, U.K., 2012.
(29) Kleinman, M. H.; Flory, J. H.; Tomalia, D. A.; Turro, N. J. *J. Phys. Chem. B* **2000**, *104*, 11472.
(30) Chen, W.; Tomalia, D. A.; Thomas, J. L. *Macromolecules* **2000**, *33*, 9169.
(31) Tomalia, D. A.; Baker, H.; Dewald, J.; Hall, M.; Kallos, G.; Martin, S.; Roeck, J.; Ryder, J.; Smith, P. *Polym. J.* **1985**, *17*, 117.
(32) Tanis, I.; Karatasos, K. *Phys. Chem. Chem. Phys.* **2009**, *11*, 10017.
(33) Lee, I.; Athey, B. D.; Wetzel, A. W.; Meixner, W.; Baker, J. R. *Macromolecules* **2002**, *35*, 4510.
(34) Jameson, D. M.; Gratton, E.; Eccleston, J. F. *Biochemistry* **1987**, *26*, 3894.
(35) Jeon, S.; Bae, S. C.; Granick, S. *Macromolecules* **2001**, *34*, 8401.
(36) Carper, W. R.; Keller, C. E. *J. Phys. Chem. A* **1997**, *101*, 3246.
(37) Levin, E. R. *Mol. Endocrinol.* **2011**, *25*, 377.
(38) Soderberg, O.; Gullberg, M.; Jarvius, M.; Ridderstrale, K.; Leuchowius, K. J.; Jarvius, J.; Wester, K.; Hydbring, P.; Bahram, F.; Larsson, L. G.; Landegren, U. *Nat. Methods* **2006**, *3*, 995.
(39) Maeda, H.; Wu, J.; Sawa, T.; Matsumura, Y.; Hori, K. *J. Controlled Release* **2000**, *65*, 271.
(40) Haag, R.; Kratz, F. *Angew. Chem., Int. Ed.* **2006**, *45*, 1198.
(41) Frasor, J.; Danes, J. M.; Komm, B.; Chang, K. C. N.; Lyttle, C. R.; Katzenellenbogen, B. S. *Endocrinology* **2003**, *144*, 4562.

DOI: 10.1021/jacs.5b05952
J. Am. Chem. Soc. 2015, 137, 10326−10335